Journal of Chromatography A, 1230 (2012) 41–47

Contents lists available at SciVerse ScienceDirect

Journal of Chromatography A

journal homepage: www.elsevier.com/locate/chroma

Capillary liquid chromatography separations using non-porous pillar array columns

Wim De Malsche[a,*], Selm De Bruyne[a,c], Jeff Op De Beek[a], Pat Sandra[b], Han Gardeniers[c], Gert Desmet[a], Frederic Lynen[b]

[a] Vrije Universiteit Brussel, Department of Chemical Engineering, Pleinlaan 2, 1050 Brussels, Belgium
[b] Laboratory for Separation Sciences, Department of Organic Chemistry, Krijgslaan 281 S4-bis, Ghent University, Ghent, Belgium
[c] Mesoscale Chemical Systems, Mesa+ Institute for Nanotechnology, P.O. Box 217, 7500 AE Enschede, The Netherlands

ARTICLE INFO

Article history:
Received 10 December 2011
Received in revised form 17 January 2012
Accepted 19 January 2012
Available online 25 January 2012

Keywords:
Pillar array column
Pharmaceutical
Micro-LC
Parabens
Phenones
Sulfonamides
Reversed phase
HILIC

ABSTRACT

We report on a series of explorative experiments wherein a non-porous pillar array column (NP-PAC) is coupled to a commercial capillary LC instrument. The performance of the system was evaluated by both non-retained and retained experiments using several types of samples. In order to minimize interfacing related dispersion, relatively large pillars (d_p = 11 μm) were defined so that a considerable depth could be achieved (50 μm), resulting in an equivalent cylindrical internal diameter of 252 μm. Connecting 20 channel tracks of 1 mm wide and 7 cm long by previously developed distributor-based turns, a large channel length (1.4 m) and volume (28 μl) could be achieved without compromising the separation performance excessively. Establishing a van Deemter curve under non-retained conditions with off-chip injection and detection, a minimal plate height of 13 μm was established, resulting in some 100,000 plates obtained in 30 min. To demonstrate the practical applicability of the NP-PAC, high pressure operation was applied to perform a number of example separations (parabens, phenones, sulfonamides, steroids and BSA digest) during a continuous operation period of 3 months wherein some 500 injections were performed. In the gradient mode, the NP-PAC approach allowed to achieve good to reasonable peak capacities (n_p = 100–140 in 50–70 min) and symmetries for both large and small solutes and for both gradient and isocratic separation modes, with figures of merit for the quantification of the peaks in the ppm range, opening more perspectives for microfluidics-based small molecule analysis.

© 2012 Elsevier B.V. All rights reserved.

1. Introduction

Miniaturization of a chromatographic technique such as HPLC is challenging as it involves downscaling of the various elements of the instrument together with the manufacturing of microscale columns, without significantly affecting key figures of merit of the technique including retention, selectivity, efficiency, sample capacity, limit of detection, linear dynamic range, repeatability, robustness, hyphenation with sample preparation and with various detectors of the equivalent HPLC analyses. If these characteristics can be reasonably preserved or improved chromatographic lab-on-a-chip approaches can be expected to find a variety of applications due to the unique related possibilities this would offer in portable devices and ensuing point of care analyses, single cell analysis, unattended continuous monitoring, process analytical technology, cost reduction, etc. Even though the ultimate goal in this research field set in the 90s by Manz was a micro-total analysis system (μTAS) [1], it has become apparent that also single used functional components can benefit from miniaturization and that reducing complexity can improve the robustness and reliability of microfluidic devices. However, linear downscaling to microfluidic methods appears more challenging than originally conceived [2,3]. This is the most apparent when column performance is compared between columns with a conventional 4.6 or 2 mm ID with micro- and nanobore columns (<2 mm and <0.5 mm ID). With the best packed micro-columns operated on state of the art nano- and micro-LC systems under the isocratic mode, it often proves difficult or impossible to achieve reduced plate heights lower of equal to 2, while this is today easily achieved in conventional HPLC and UHPLC application over broad retention ranges [4]. As there is essentially no relationship between column diameter and expected column performance, except for the extremely narrow columns where the ratio of column ID to particle size becomes very small (<10) where wall effects can dramatically reduce the performance, the loss of performance should be related to the increasing relevance of extra-column voids and to less efficient column packing strategies. For these reasons, most microfluidic chromatographic applications today typically employ gradient analysis, which allows

* Corresponding author. Tel.: +32 2 629 33 18; fax: +32 2 629 32 48.
E-mail address: wdemalsc@vub.ac.be (W. De Malsche).

0021-9673/$ – see front matter © 2012 Elsevier B.V. All rights reserved.
doi:10.1016/j.chroma.2012.01.060

refocusing of the solutes at the head of the column and minimizes peak broadening related to the injection process [4–6]. Additionally the majority of micro and nano-LC methods involve the analysis of larger biomolecules relevant to genomic and proteomic research [7–9], solutes for which it is difficult to achieve satisfactory peak shapes and high peak capacities in the isocratic mode. By contrast, when analyzed in the gradient mode, excellent peak capacities are observed [10]. This suggests that, next to the partition phenomena, also an (at least) partial precipitation/re-dissolution effect takes place (leading to a so-called on-off retention mechanism). The direct insertion of the column aperture in the ESI-MS source allows benefiting maximally from the enhanced ionization effects of micro-flows with minimal extra column peak broadening [11,12]. However, current microfluidic methods are rarely applied in validated environments, because of the poor method reproducibility and lack of ruggedness which are often experienced.

The use of micro-fabricated pillar array columns in micro and nano-LC could, as originally proposed by Regnier [13], introduce significant benefits in terms of column reproducibility and performance and could broaden the applicability range to a much broader variety of molecules. In previous work on pillar array columns [13–16], the emphasis was mainly on the chip design aspects and the inherent chip performance, and the injection and detection were therefore usually carried out on-chip. This strategy allowed e.g. for the on-chip injection and detection of sub-nl sample plugs in a 150 μm wide and 7.2 μm deep channel with a total length of 3.1 m and a total column volume of 2 μl, constructed by 2–5 cm channel tracks that were interconnected by flow distributors. Detecting the band dispersion at the end of this channel that contained 5 μm diameter pillars with a spacing of 2.5 μm, about 1 million theoretical plates could be achieved in less than 20 min (for a non-retained component) [17]. Thus far, pillar array chips have to the best of our knowledge never been tested in a commercial capillary LC system yet.

In the present contribution, we report on our first attempts to design a pillar array chip so that it can be directly coupled to a commercial micro-LC, as a replacement of the capillary columns that are normally used. To this end, a much larger channel volume (28 μl) was aimed at in comparison with previous studies (e.g., 2 μl in [17]) by using wide (1 mm) channels and larger pillars (11 μm), allowing for a larger pillar height (50 μm) than in the above mentioned study [17], in order to minimize system related dispersion.

The system was tested for a number of different isocratic and gradient separations with relevance in the field of pharmaceutical, cosmetic, food and environmental.

2. Experimental

2.1. Materials

HPLC grade water and HPLC-S gradient acetonitrile were obtained from Biosolve (Valkenswaard, The Netherlands) Spectrophotometric trifluoroacetic acid (TFA), methanol, uracil, thymine, adenine, cytosine, toluene, ammonium formate, the phenones parabens, sulfonamide pharmaceuticals and steroids were purchased from Sigma–Aldrich (Bornem, Belgium). Formic acid (85%) was purchased from Belgolabo (Overijse, Belgium). A BSA tryptic digest was purchased from ProteaBio (500 pmol) and diluted with 100 μl of 0.10% TFA in 98/2 (vol.%/vol.%) H_2O/ACN.

2.2. Chip fabrication and design

A 1.4 m long and 1 mm wide pillar-array channel (11 μm diameter pillars, inter-pillar distance 2.5 μm) was patterned using normal UV photolithography (photoresist, Olin 907-12), followed by a dry etching step (Adixen AMS100DE, Alcatel Vacuum Technology, Culemborg, The Netherlands) to etch the 200 nm thick SiO_2 hard mask underneath. Next, the capillary channels were defined by subsequent mid-UV lithography, etching of the SiO_2 layer by a Bosch-type deep-reactive-ion etching step (Adixen AMS100SE) reaching a depth of 80 μm. After this, the resist was removed by oxygen plasma and nitric acid, and the pillars defined in the SiO_2 mask (and also the already defined and partly etched capillary groove) were subsequently Bosch etched to reach a depth of 50 μm (and the capillary channel a total depth of about 130 μm).

A diverging array of radially stretched diamond-shaped pillars with a width-over length aspect ratio of 5 was placed at the capillary-pillar channel interface to ensure a good flow distribution over the entire width of the pillar-array column (see Fig. 1). Given the limited length per track, the channel was constructed by interconnecting 20 channel tracks of 1 mm wide and 7 cm long by distributor-based turns. In the adopted design, each channel track is preceded and followed by a flow distributor [18,19] and the different tracks are connected via a narrow (10 μm) turn structure, an approach that was introduced in [17,18] but with much narrower channels (150 μm) than in the current study (1 mm).

The microfluidic channels were subsequently sealed with a Pyrex wafer (thickness 0.5 mm), anodically bonded to the silicon using an EVG EV-501 wafer bonder (EV Group Inc., Schaerding, Austria). Next, the chip was diced (100 μm deep) from both sides of the wafer and subsequently cleaved, exposing the channels to insert the interfacing capillaries (108 μm OD and 40 μm ID, Polymicro Technologies, Phoenix, Arizona, United States) into. Subsequently, the capillaries were inserted in the grooves and sealed by epoxy glue. A C8 hydrophobic coating was applied on the non-porous silicon substrate by means of a liquid-phase coating procedure consisting of the following steps. First, the microchannels were flushed with methanol for 1 d and anhydrous toluene for 1 d. A solution of 5% octyldimethylchlorosilane (C8) in anhydrous toluene was pumped through the channel for 72 h at room temperature. Afterwards, the channels were flushed with anhydrous toluene for 1 d and with methanol for 1 d.

2.3. Methods

Experiments were performed on a Ultimate 3000 system (Dionex, Amsterdam, Netherlands) equipped with a quaternary pump, autosampler, column oven compartment, variable wavelength detector and with a 1/300 flow splitter to percolate microliter/min flow rates in a controlled way through columns. The detector was equipped with a 3 nl flow cell to minimize extra column peak broadening. The capillaries connected to the inlet (directly connected to the injection valve) and to the outlet (coupled to a zero-dead-volume-connection) had an i.d. of 40 μm and respective lengths of 55 and 24 cm (with volumes of respectively 0.7 and 0.3 μl). The capillary connected with the other size of the zero-dead-volume-connection and running through the flow cell (optical path 1 mm) had an i.d. of 20 μm and a length up to the cell of 35 cm (0.3 μl).

In all applications sample volumes consisted of 40 nl, introduced on the chip via the partial loop injection volume mode, except for the tryptic digest samples which were injected in the full loop mode (loop volume 1 μl). The stock solutions of the nucleotides were dissolved in 0.2 M NaOH and subsequently the pH was adjusted with 0.2 N HCl. The stock solutions of the toluene, phenones, parabens and steroids were prepared in acetonitrile. Stock solutions of the individual sulfonamides were prepared in methanol. Standard solutions for the RPLC analyses were prepared by appropriate dilutions of the stock solutions in water/acetonitrile (90/10). The BSA tryptic digest was dissolved in water (0.1% TFA)/acetonitrile (98/2).

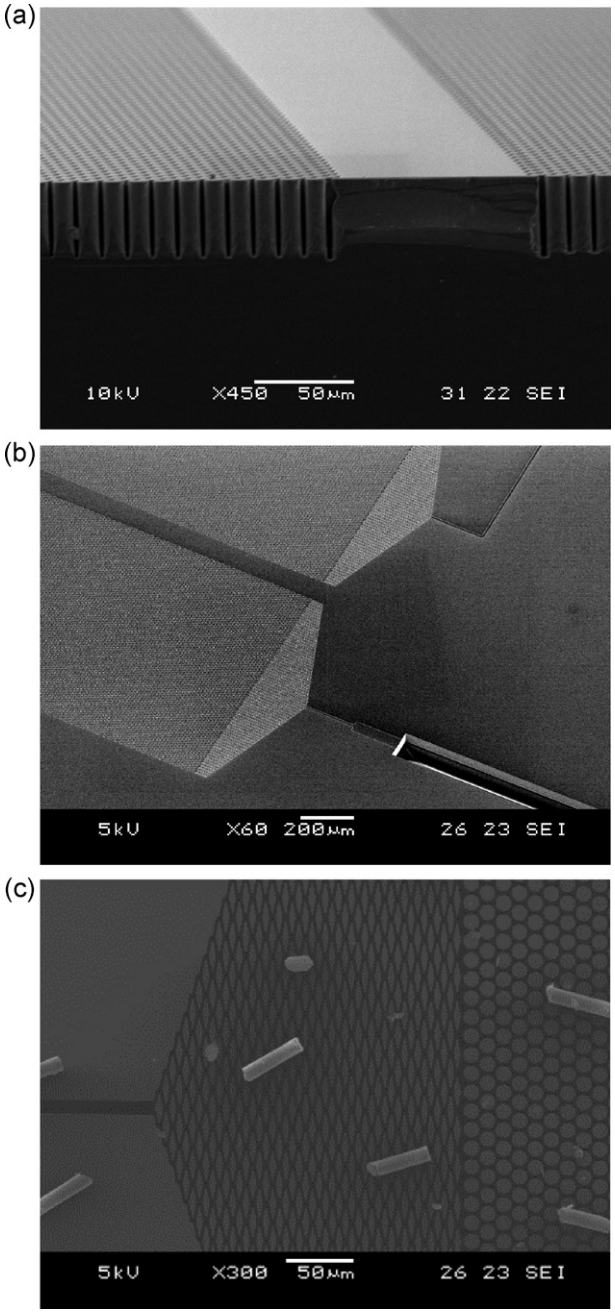

Fig. 1. SEM images of (a) cross-section of silicon bottom wafer showing two adjacent channel tracks and (b) entrance region, including the groove (1) in which the connection capillary is inserted, followed by a flow distributor zone (2), and the two first lanes (3 and 4) of the pillar bed. (c) Close-up of the flow distributor. The broken pillars on top of the pillar bed are cause by cleaving the sample for SEM imaging.

2.4. High-pressure and low dead volume connection

To allow for a high-pressure operation, the size of the connection capillaries was reduced so that special receptor grooves with reasonable depths (see (2) in Figs. 1b and 2a) could be etched close to the in- and outlet of the channel to glue in the connection capillaries over a distance of about 5 mm, see also [17]. The grooves extend until the inlet distributor, which allows the close placement of the capillary to the distributor, hence minimizing the occurrence stagnant zones. To fix the capillaries, epoxy glue was applied at the interface of the chip while the capillary was already inside. Subsequently, the capillary was moved back and forth to wet the entire outer surface of the capillary, up to the terminal fraction (Fig. 2).

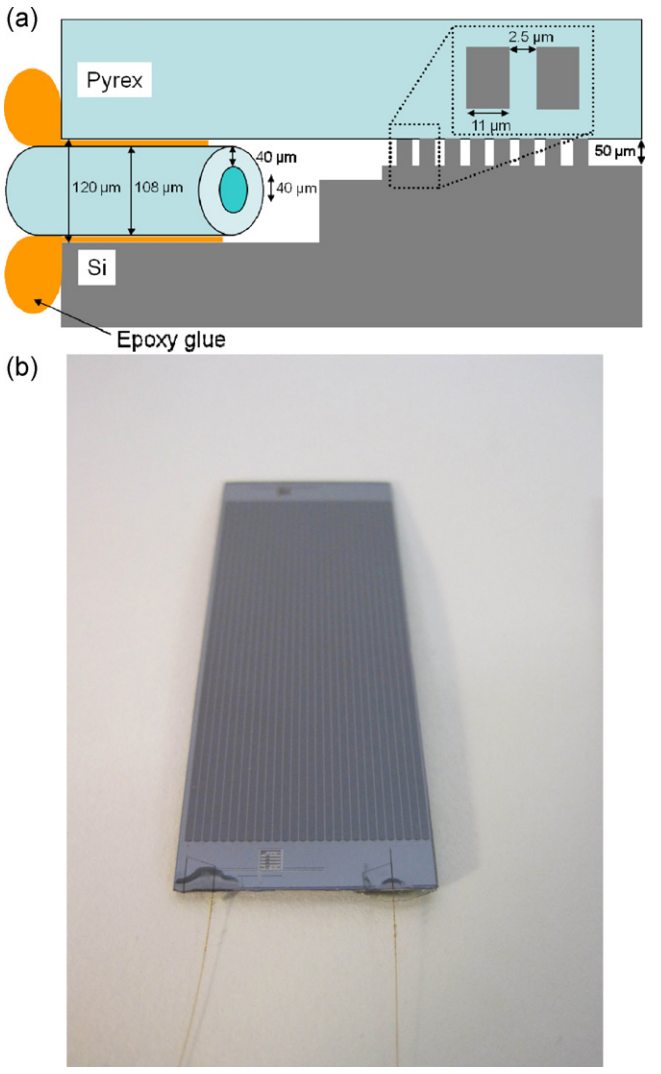

Fig. 2. (a) Schematic drawing of the procedure used to glue the fused-silica connection capillaries into the pillar array chips and (b) optical image of the final assembly, showing the in- and outlet capillary and the adjacent 7 cm long tracks making up the 1.4 m long separation channel (the chip shown in this image contains 28 channel tracks instead of the 20 tracks used throughout this study).

This procedure allows a leak-tight operation for the applied pressures (tested up to the maximum of the pump, i.e., 350 bar). The final assembly is shown in Fig. 2b. For the evaluation of the reproducibility of the connection, 3 different 25 cm long channels were tested. Applying off-chip injection, the RSD of the on-chip obtained peak width was evaluated with a fluorescence microscope, coupled with an air-cooled CCD fluorescence camera (Hamamatsu Photonics K.K., Japan). A Hg-vapour lamp was used to excite the fluorescent C440 coumarin dye in the UV. The peak intensity profiles were subsequently analyzed using the accompanying Simple PCI® image analysis software. On-column chromatograms were obtained by averaging a row of pixels and plotting its values in function of time.

3. Results and discussion

3.1. System characterization

As the goal of this work was to demonstrate the practical applicability of NP-PAC's to address relevant separation problems, a chip carrying a PAC was designed such that it could be directly interfaced to a commercial micro-/nano-LC system and use the external

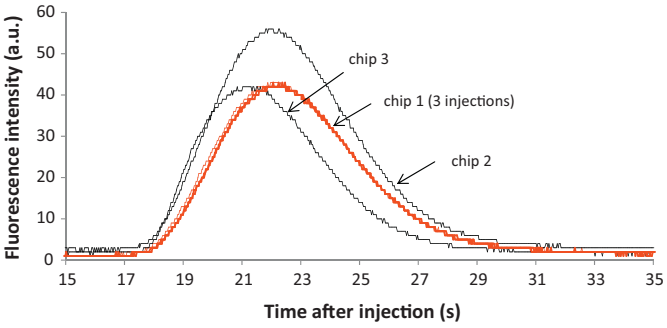

Fig. 3. Evaluation of the reproducibility of the glue procedure. Sample plugs of 200 nl Coumarin C440 were injected off-chip (flow rate 1.5 μl/min) in 3 different 25 cm long test chips and subsequently recorded on-chip at the inlet of the respective channels using a fluorescence microscope equipped with a CCD camera. The readouts were obtained by averaging a row of pixels and plotting its values in function of time. The RSD of the peak width is 9%. The RSD of the peak width for repeated injections for each chip is smaller 1% (depicted for chip 1).

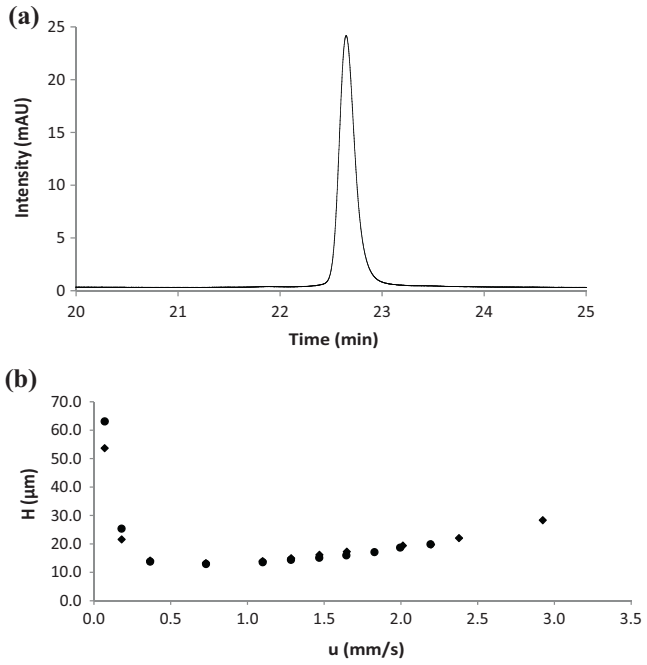

Fig. 4. (a) Chromatogram of an injected band of toluene (100 ppm) in acetonitrile/water 50/50; inj. vol.: 40 nl, detection UV @ 210 nm under non-retained conditions (1.5 μl/min) and (b) van Deemter curve obtained by injecting 30 ppm of coumarin 440 in 70/30 MeOH/H_2O (flow rates between 0.1 and 4 μl/min), detection @ 350 nm, injection volume 40 nl. The diamond symbols were obtained by increasing the flow rate, vice versa for the circular symbols.

pumping, injection and detection modules of the instrument. In previous studies of our group on pillar array columns (NP-PAC), the detection and injection were always performed on-chip. In order to create a satisfactory detection sensitivity, this on-chip detection was limited to fluorescently labeled molecules, whereas UV detection is needed if one is to solve real-world separation problems. Similarly, also the injection was done on-chip, via an integrated microfabricated injection loop [14]. This approach requires a second pump to pump the sample in the supply channels. Despite that this approach allowed to reproducibly inject sub-nl sample volumes, the procedure requires a rather complex assembly and is currently not robust enough to develop separation protocols on a systematic fashion in an analytical lab environment. Hence the need to also switch to a commercial off-chip injector.

Key to any successful off-chip injection and detection scheme is the minimization of the extra-column band broadening. This, amongst other demands, requires that the column volume is sufficiently large compared to that of the rest of the system. Given that the columns that were used during our on-chip studies had a relatively small volume, we opted in the present study to fabricate a very long channel (1.4 m) to maximize the column volume. Relatively large pillars of 11 μm diameter with a spacing of 2.5 μm (40% porosity) were chosen, as a compromise between the possibility to achieve a reasonable plate height and a maximal channel volume (the etch depth that can be achieved while maintaining an acceptable verticality scales with the feature size).

Etching the pillars 50 μm deep, a pillar channel volume of 28 μl could was achieved. Compared to a cylindrical capillary of the same length, this would correspond to a capillary with an internal diameter of 252 μm. Fig. 1a shows the cross-section of two adjacent separation channel tracks, allowing to appreciate the high vertical aspect ratio of the inter-pillar gaps.

In order to evaluate the chip-to-chip reproducibility of the glued connection zone, off-chip injection of coumarin C440 (1 mM in methanol) in a (25 cm long) test channel (flow rate: 1.5 μl/min, mobile phase methanol) was executed using an in-house built automated injection loop/valve system and on-chip detection was performed with a fluorescence microscope (see Fig. 3), allowing an off-chip injection nearby the fluorescence microscopy setup via a 40 cm long and 40 μm i.d. capillary. Determining the RSD of the width (obtained at 13.4% peak height) of the injected plug with an injection volume of 200 nl, a value of 9% was obtained (the intra-chip RSD of the injection system itself was always <1%, 3 injections are depicted for chip 1 in Fig. 3). Regarding the wafer-scale uniformity of the feature definition, it has been recently shown by on-chip measurements [17] that the local plate height within large wafer surfaces is constant even when the column runs across the entire wafer (excluding the border region). These wafer-scale variations are generally larger than wafer-to-wafer variations in state-of-the-art cleanrooms when dry etching procedures are involved.

In order to evaluate the native performance of the pillar bed coupled with the injector and detector, first a number of non-retained experiments were performed. In Fig. 4a, a typical chromatogram of toluene injections is shown at different flow rates. At the optimal flow rate (1.5 μl/min), the peak width corresponds to 102,000 theoretical plates (H_{min} = 13.4 μm). Slightly smaller H_{min}-values were obtained for coumarin C440 in methanol (from 0.1 to 4 μl/min).

Fig. 4b shows the corresponding van Deemter curve. In previous on-chip experiments carried out on 5 cm long non-porous channels [20] with similar dimensions (10 μm diameter pillars, porosity 40%, 19 μm deep), a minimal reduced plate height of 0.2 was obtained when only the central part of the channel was taken into account. For the presently considered pillar size (11 μm), this would correspond to a plate height of about 2 μm. Obviously, the plate heights obtained in the current study are dramatically larger. It is suspected that this strong loss in performance is due to a combination of dispersion at the turns, sidewall effect, dispersion at inlet- and outlet connections, in the connection capillary and at the connection piece interfacing the chip capillary with the detector capillary. In a separate future study, the extent of all these dispersive sources as well as the chip-to-chip reproducibility will be investigated by building a setup that contains both a fluorescence microscope and an HPLC system to study the peak variance at all these critical locations.

3.2. HILIC application

Although the unretained column performance measurements shown above experiments are useful to quantify the intrinsic band broadening properties of this type of columns when coupled to a commercial instrument, they have little or no practical use. In

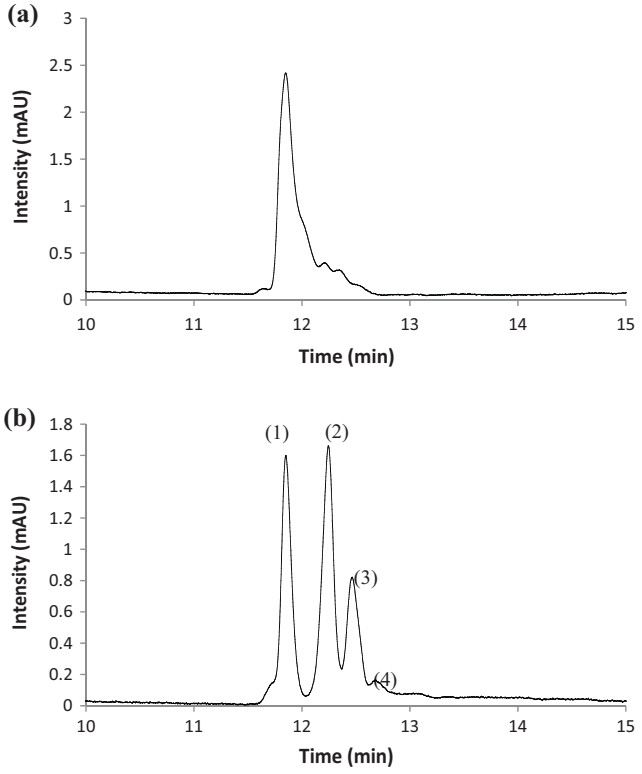

Fig. 5. HILIC experiment sample: (1) thymine (25 ppm), (2) uracil (25 ppm), (3) adenine (25 ppm), (4) cytosine (25 ppm). Mobile phase: acetonitrile and 100 mM ammoniumformate buffer (pH 6.6), inj. vol.: 40 nl, detection UV @ 210 nm. Flow rate 2.4 μl/min (a) 90% AN and (b) 98% AN. Peak (1) corresponds to $N_{50\%}$ = 77,663 plates.

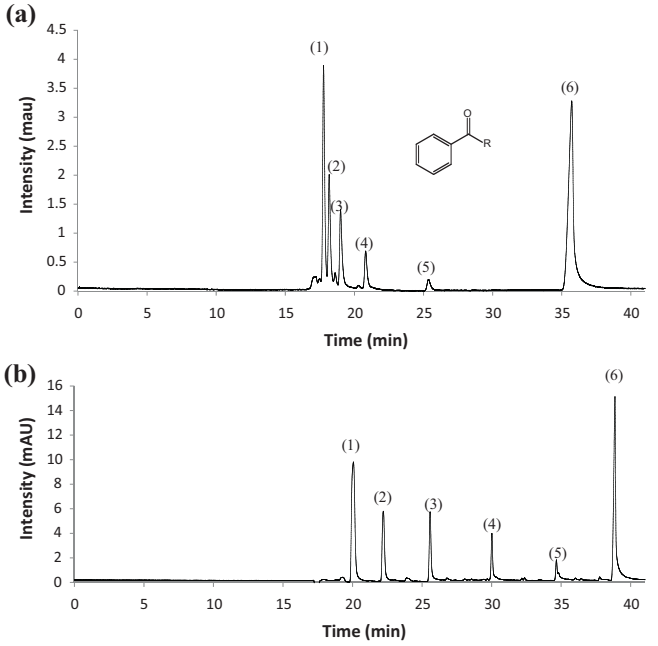

Fig. 6. (a) Isocratic separation of a phenone series (acetophenone (1), propiophenone (2), butyrophenone (3), valerophenone (4), hexanophenone (5), heptanophenone (6)), 2 μl/min, 20% MeOH. Detection: UV @ 254 nm, inj. vol.: 40 nl, 30 ppm each, except (6): 100 ppm. Plate numbers obtained for selected peaks obtained at different channel heights are (1): $N_{50\%}$ = 77,663, $N_{32.5\%}$ = 70,969, $N_{13.4\%}$ = 64,371; (4): $N_{50\%}$ = 59,863, $N_{32.5\%}$ = 53,361, $N_{13.4\%}$ = 39,204; (6): $N_{50\%}$ = 51,604, $N_{32.5\%}$ = 47,800, $N_{13.4\%}$ = 33,536. (b) Gradient separation of phenone series 0–90% MeOH in 60 min (A is water).

the next stage, a series of retained component experiments was therefore initiated. Given the emerging popularity of hydrophilic interaction liquid chromatography (HILIC) for the analysis of polar and often ionic solutes [21,22], it was considered worthwhile to investigate the retention and separation performance of the native silicon oxide layer surface area of the non-porous chip in the HILIC mode. For this purpose, a mixture of typical HILIC test compounds (thymine, uracil, adenine, cytosine) was analyzed on the chips under HILIC conditions of decreasing eluotropic strength, in the isocratic mode. As can be seen in Fig. 5, retention is increasing as a function of decreasing water content in the mobile phase, confirming the pursued HILIC effect. Although, to the best of our knowledge this is the first time HILIC could be applied in this type of microfluidic studies, acceptable retention factors, acceptable peak capacities or large sample capacities could not be obtained in this way.

3.3. Reversed phase separations

The chips were subsequently coated with octyldimethyl chlorosilane, to create a thicker retentive layer in the reversed phase mode compared to the very thin predominantly hydrophilic layer close to the surface in the HILIC mode. The coated chips were subsequently evaluated with various reversed phase test samples. In Fig. 6a, an isocratic separation of a mixture of 6 phenones is demonstrated in an aqueous mobile phase containing MeOH. Although the chip surface is non-porous, and therefore only has a limited retention surface, a satisfactory retention was already obtained at 20% of the organic modifier, leaving room to further increase the retention by further decreasing the MeOH percentage for the more polar solutes. The concentration of the last eluting solute was increased (100 ppm) to illustrate the peak shape of a retained compound in a better way. Although some tailing is observed, which can be related to the extra column peak broadening effects, these effects where not overwhelming and were not affecting the peak capacity too much.

In order to investigate if the asymmetry was related to injection peak broadening rather than to post column voids, gradient separations were performed (Fig. 6b). This was done to focus the hydrophobic solutes at the head of the column to suppress the pre-column peak broadening. As expected, the bands are now much narrower (due to the gradient elution effect), but the tailing remains, indicating the tailing observed in the isocratic experiments mainly originates in or after the separation channel. Analyzing the isocratic elution bands at different peak heights, it is clear that the bands are considerably wider at their bottom part than over their top fraction (e.g., for the middle peak (4), $N_{50\%}$ = 59,864, $N_{32,5\%}$ = 53,361 and $N_{13.4\%}$ = 39,204). The strong tailing is indicative of a strong mixer effect occurring at the end of the column [23], in which case we suspect that this mixing occurs in the coupling piece used in between the connection capillary of the channel and that of the detector. Another plausible cause would be the occurrence of a secondary adsorption mechanism on the pillars, or an overloading effect. The amounts of sample that needed to be injected in order to obtain a good S/N-ratio were fairly large. Given the limited retention surface (only outer pillar surface available) mass overloading might certainly occur.

Taking the separation of a paraben mixture as an example, Fig. 7 illustrates how these solutes also allow for the same type of gradient optimization of the elution pattern and the separation selectivity. Whereas for an acetonitrile gradient between 10 and 90% the peaks in the beginning of the chromatogram elute relatively close to each other, the peaks can be spread out much more uniform by switching to a 0–90% gradient. It can be seen that the

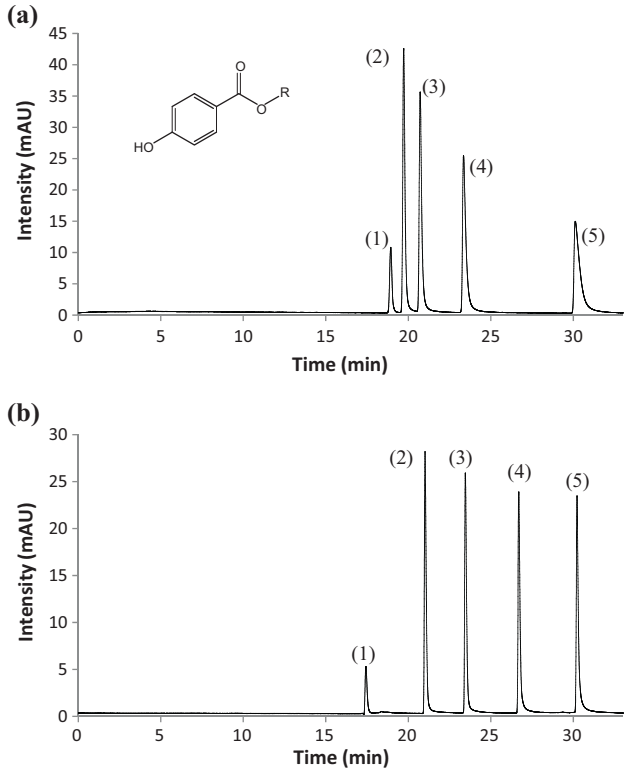

Fig. 7. Paraben gradient separations. Sample: uracil (1), methylparaben (2), ethylparaben (3), propylparaben (4), butylparaben (5), flow rate: 2 μl/min. Detection: UV @ 254 nm, inj. vol.: 40 nl, 30 ppm each (a) 10–90% AN in 60 min and (b) 0–90% AN in 60 min.

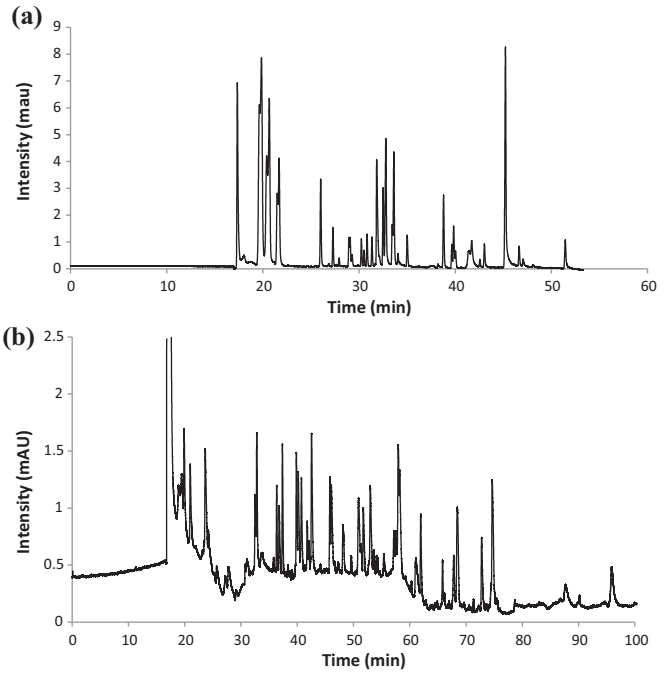

Fig. 9. (a) Gradient separation of steroids. Conditions: A: water + 0.1% TFA, B: acetonitrile, 0–100% B in 60′, flow rate: 2 μl/min, inj. vol.: 1 μl. Detection: UV @ 210 nm sample, 30 ppm each. The average peak capacity (based on 3 large peaks at the end of the chromatogram and determined at half height) is P_c = 125 and (b) BSA digest. The average peak capacity is P_c = 140.

retention was decreased for the most polar solutes and increased for the more hydrophobic ones.

As generic reversed phase LC methodologies today typically employ mobile phases with added volatile acids, such conditions were also investigated on the chips for the analysis of a number of pharmaceutical structures. The addition of acids protonates residual silanol functions, reducing tailing of basic and polar analytes in general. Weakly acidic solutes are hereby protonated and therefore more retained in RPLC, whereas the protonated weakly basic groups are forming an ion pair with the alkylate counter ion, which allows neutralization and therefore retention in this chromatographic mode. As an example of this approach, Fig. 8 shows a gradient analysis of a mixture of sulfonamide drugs using 0.1% acetic acid as additive to the water. As the same elution order was observed as previously described for the analysis of this type of solutes with conventional RPLC [24], it can indeed be concluded that under these conditions few residual polar active sites remain, as otherwise the most polar solutes would have been more strongly retained. Moreover, the peak shapes are somewhat better compared to the more hydrophobic phenones and parabens, although this might also have been caused by a different position of the coupling capillaries in the union piece used to connect the chip to the detector during the period the experiments shown in Fig. 8 were conducted.

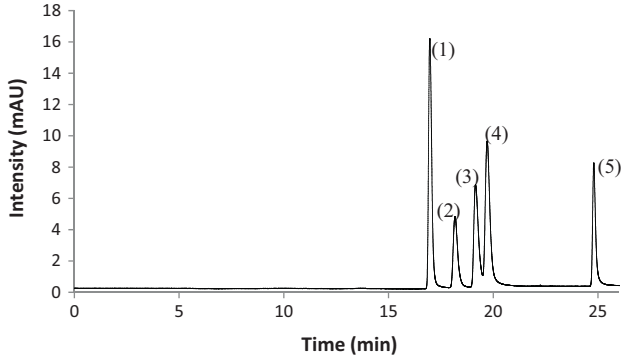

Fig. 8. Gradient separation of the sulfonamides sulfaguanidine (1), sulfamerazinine (2), sulfamethazine (3), sulfamethaxozole (4), sulfadimethoxin (5). Conditions: A: water + 0.1% formic acid, B: acetonitrile flow rate: 2 μl/min. Detection: UV @ 254 nm, inj. vol.: 40 nl, 30 ppm each, 100% A (10 min), 100% A → 60% A (50 min).

The use of acidic gradients to obtain optimal peak shapes, and therefore peak capacities, was further explored by the analysis of a more mixtures composed of 37 steroids (Fig. 9) and of a tryptic digests of bovine serum albumin (BSA), whereby trifluoroacetic acid (TFA) was used as ion pair former. In both cases, a reasonably good peak capacity was obtained, despite the relatively small elution window. Using the average peak capacity definition of Neue [25], the first chromatogram corresponds to a peak capacity of about 125, whereas the second chromatogram corresponds to a peak capacity of 140. According to the kinetic plot extrapolation presented in Fig. 2 of [26], commercial packed bed and monolithic capillary columns need about 30 min to obtain such peak capacities. This is not much faster than the times needed with the PAC in the present study, especially when considering that a relatively large pillar size was used.

As these values could be achieved within reasonable analysis times and for very small injection volumes, one can conclude that the NP-PAC can today already be effectively applied in a number of RPLC applications in commercial micro-LC instrumentation.

Finally, it should be noted that the experiments were carried out over a period of 3 months (corresponding to roughly 500 injections, followed by a flush step), using the same column. No clogging problems occurred, not even under the realistic test conditions employed in the present study.

4. Conclusions

In this contribution, the practical use of non-porous pillar array columns was investigated by directly coupling the chips carrying the column to a commercial nano-/micro-LC system. A maximal chip performance was pursued by employing well-established principles used in HPLC method development, such as the addition of volatile acids as ion pair formers, and the use of gradients to refocus hydrophobic analytes at the head of the column. In this way, and taking into account that fairly large pillar dimension (11 μm) were used, satisfactory peak capacities in the order of 100–140 could be obtained for the separation of mixtures of phenones, parabens, sulfonamides, steroids and tryptic digests. The peak shapes however often displayed a severe tailing, which is most probably caused by the dead mixing zones created at the coupling between the chip capillary and the detector capillary. Detection sensitivities comparable to what is achievable with HPLC-UV were obtained for all types of analyzed sample, although only nanoliter volumes were injected (except for the tryptic digest sample). Future research should aim at the development of improved connections between the chip and the capillary connected to the detector.

Acknowledgements

The Flemish Research Foundation (FWO-Vlaanderen) is kindly acknowledged for funding the purchase of the micro-LC system and for financially supporting WDM in this research.

References

[1] A. Manz, Y. Miyahara, Y. Watanebe, H. Miyage, K. Sato, Sens. Actuators B 1 (1990) 249.
[2] H. Poppe, J. Chromatogr. A 778 (1997) 3.
[3] J.C.T. Eijkel, A. van den Berg, Electrophoresis 27 (2006) 677.
[4] F. Lestremau, D. Wu, R. Szücs, J. Chromatogr. A 1217 (2010) 4295.
[5] D. Guillarme, S. Rudaz, C. Scheling, M. Dereux, J.-L. Veuthey, J. Chromatogr. A 1192 (2008) 103.
[6] S. Eeltink, S. Dolman, F. Detobel, R. Swart, M. Ursem, P.J. Schoenmakers, J. Chromatogr. A 1217 (2010) 6610.
[7] D. Tao, L. Zhang, Y. Shan, Z. Liang, Y. Zhang, Anal. Bioanal. Chem. 399 (2011) 229.
[8] T.J. Causon, R.A. Shellie, E.F. Hilder, J. Chromatogr. A 1217 (2010) 3765.
[9] L.R. Snyder, M.A. Stadalius, M.A. Quarry, Anal. Chem. 55 (1983) 1412.
[10] H. Yin, K. Killeen, R. Brennen, D. Sobek, M. Werlich, T. Van De Goor, Anal. Chem. 77 (2005) 527.
[11] J. Rozenbrand, W.P. Van Bennekom, J. Sep. Sci. 34 (2011) 1934.
[12] H. Toll, R. Wintringer, U. Schweiger-Hufnagel, C. Huber, J. Sep. Sci. 28 (2005) 1666.
[13] B. He, N. Tait, F. Regnier, Anal. Chem. 70 (1998) 3790.
[14] W. De Malsche, H. Eghbali, D. Clicq, J. Vangelooven, H. Gardeniers, G. Desmet, Anal. Chem. 79 (2007) 5915.
[15] L.C. Taylor, N.V. Lavrik, M.J. Sepaniak, Anal. Chem. 82 (2010) 9549.
[16] C. Aoyama, A. Saeki, M. Noguchi, Y. Shirasaki, S. Shoji, T. Funatsu, J. Mizuno, M. Tsunoda, Anal. Chem. 82 (2010) 1420.
[17] W. De Malsche, J. Op De Beeck, S. De Bruyne, H. Gardeniers, G. Desmet, Anal. Chem. (2012), doi:10.1021/ac203048n.
[18] S.K. Griffiths, R.H. Nilson, Anal. Chem. 73 (2001) 272.
[19] J. Vangelooven, G. Desmet, J. Chromatogr. A 1217 (2010) 6724.
[20] W. De Malsche, H. Gardeniers, G. Desmet, Anal. Chem. 80 (2008) 5391.
[21] D.V. McCalley, J. Chromatogr. A 1171 (2007) 46.
[22] S. Louw, F. Lynen, M. Hanna-Brown, P. Sandra, J. Chromatogr. A 1217 (2010) 514.
[23] A. Felinger, Data Analysis and Signal Processing in Chromatography, Elsevier, Amsterdam, The Netherlands, 1998.
[24] T. Gorecki, F. Lynen, R. Szucs, P. Sandra, Anal. Chem. 78 (2006) 3186.
[25] U.D. Neue, J. Chromatogr. A 1079 (2005) 153.
[26] A. Vaast, K. Broeckhoven, S. Dolman, G. Desmet, S. Eeltink, J. Chromatogr. A (2011), doi:10.1016/j.chroma.2011.07.089.